



Fast and Efficient Methylene Blue Photodegradation Process Using Natural Iron Oxide as Catalyst in the Dark and Under Irradiation

K. Benhamouda, T. Sehili, K. Djebbar

Laboratoire des Sciences et Technologies de l'Environnement (LSTE), Université Constantine1, Algérie.

E-mail: benhamoudakarima@umc.edu.dz

Received 10 May 2016,

Revised 10 Jul 2017,

Accepted 13 Jul 2017

Keywords

- ✓ Natural iron oxide;
- ✓ Catalysis;
- ✓ Photodegradation;
- ✓ Methylene Blue;
- ✓ Aqueous solution

benhamoudakarima@umc.edu.dz

Abstract

Heterogeneous photodegradation of Methylene Blue (MB) in the presence of Natural Iron Oxide (NIO) was investigated in the solution medium. Five methods for characterizing the NIO were employed: X-ray diffraction (XRD), X-ray fluorescence and Brunauer–Emmett–Teller (BET) analysis, Raman and scanning electron microscopy (SEM). These analyses showed that the NIO consists essentially of hematite (89 %). To dissolve iron from the NIO we have used citric acid, tartaric and oxalic acid and the results confirmed that the Fe(II) was obtained in the presence of oxalic acid (OA). Under UVA light, the most efficient degradation of MB was achieved with the OA which 100 % degradation ratio was reached within 90 minutes. The effect of various parameters such as concentration of dye, concentration of OA, pH and type of radiation (solar or UV radiation) on the NIO/OA process were investigated. The process was closely related to the concentration of oxalate and to the pH value as well. The optimal MB photodegradation was found with 4×10^{-3} M of OA at pH = 3. Use of 2.0 % of *ter*-butanol, as a scavenger of hydroxyl radicals, confirmed the main involvement of these entities in the MB's photodegradation mechanism.

1. Introduction

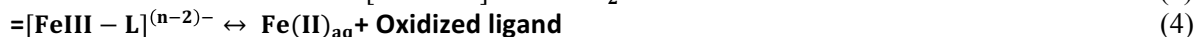
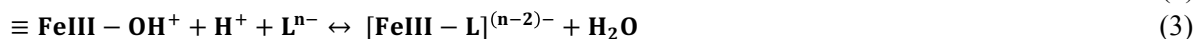
Dye pollutants produced widely from chemical colorization process in manufactories and mainly issue from the textile industries are becoming a major source of environmental contaminations [1,2]. It is considered as a high source of non-aesthetic pollution which has a significant influence on host infection of the aquatic ecosystems. Furthermore, these dyes are not biodegradable and under anaerobic conditions they could be transformed into carcinogenic aromatic amines [3,4].

Advanced oxidation technologies for wastewater treatment have attracted attention due to the generation of powerful oxidizing species ($\bullet\text{OH}$, $\text{O}_2\bullet^-$, etc.). Among this process, photo-Fenton and photo-Fenton-like reactions have been extensively used to degrade dyes [5,6]. However, in natural aquatic environment, the application of these processes for the degradation of pollutants is limited because of the instability of hydrogen peroxide and a narrow pH working range. These disadvantages have made the development of a heterogeneous Fenton and like-Fenton systems imperative.

Many studies report that the heterogeneous Fenton and Fenton-like processes can be set up using hydrogen peroxide and supported or immobilized catalysts [7,8] or in the presence of iron oxide and carboxylic acids [9]. However, the synthesized catalysts take time and require chemical reagents and expensive characterization analyzes. That is why, at our research laboratory, we thought about substituting them by natural catalysts.

Among the wide variety of solid natural catalysts, iron oxides, including hematite, maghemite, goethite and lepidocrocite show semiconductor properties with a narrow band gap of 2.0–2.3 eV and interesting catalytic activities under solar irradiation [10,11]. These compounds can form strong complex with polycarboxylates such as citrate, tartrate, and oxalate and create a photo-Fenton-like process because they enhance the dissolution of iron in natural water through photochemical processes. In the solution, the reaction of polycarboxylates with iron oxides leads to the formation of surface-bound Fe(II) species through three steps: (i) adsorption of organic ligands on the iron oxide surface, (ii) non reductive complexation, and (iii) reductive complex [12,13]. To

transfer the Fe(II) from the solid iron oxide to the water. Firstly, an electrical double layer is established at the interface by acid ionization and protonation of oxygen when iron oxide particles suspend in polycarboxylic acid as shown in Eqs. (1) and (2). Secondly, the formed surface hydroxyl groups become active sites for subsequent adsorption of organic ligands as described by Eq. (3). Thirdly, during the leaching process, on the oxide surface, Fe(III) reduces to Fe(II) due to electron transfer from the adsorbed carboxylic acid [14]. The reduction of structural Fe(III) to Fe(II) destabilizes the coordination sphere of the iron both as a result of the loss of charge and because of the larger size of the Fe(II) and thus induces detachment of iron as Fe(II) Eq. (4):



The presented work aims to study the degradation of MB in the presence of NIO and different concentration of oxalic acid (OA), citric acid (CA) and tartaric acid (TA) in the dark and under irradiation. The effects of various parameters, such as; initial concentration of OA, initial concentration of dye, pH values and type of irradiation on the photocatalytic degradation of MB by NIO/OA process were studied and analyzed to find out the optimum treatment conditions.

2. Experimental and methods

MB was supplied by Reidel-de Haën (> 99%). Sodium hydroxide (98%, Carlo Erba Reagenti). Sulfuric acid, ammonium acetate and sodium acetate (98%, 98%, 99%, Panreac). 1,10-phenanthroline (>99%, Fluka), perchloric acid, OA, CA and TA (98%, 99.5%, 100% and 100% respectively, Prolabo), the different solutions were prepared using ultrapure water on a Millipure apparatus. Fig. 1 represent the spectrum UV-Vis of MB.

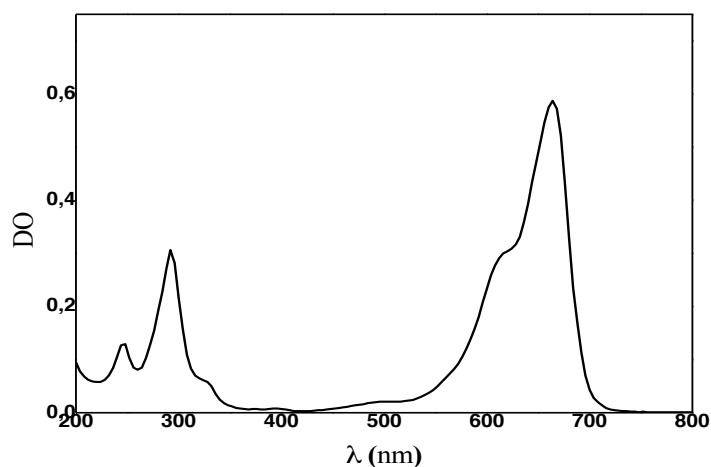


Figure 1. Spectrum UV-Visible of MB (10^{-5} mol.L $^{-1}$)

2.2. Procedure and analysis

The irradiation experiments were carried out in a self-constructed Pyrex photoreactor (diameter of 2 cm) with a cooling water jacket placed in an elliptical stainless steel chamber. A fluorescent lamp (Philips TLAD 15W/05), which dominantly emits radiation at 365nm was used. Light intensity ($I = 0.45$ mW cm $^{-2}$) was measured using a radiometer type VLX 3W. The lamp and the reactor are on both focal axes of the elliptical chamber. The reaction temperature was kept at 20 ± 1 °C by cycling water. The irradiated solutions and suspensions were magnetically stirred during whole experiments. The suspensions of MB (10^{-5} M) and 1 g.L $^{-1}$ of NIO were stirred in the dark for 30 min before irradiation to establish adsorption/desorption equilibrium. The particles of NIO were removed after irradiation by filtration through cellulose acetate (Millipore 0.45 μ m). The concentration was monitored by measuring the absorbance at $\lambda_{max} = 664$ nm using a UV-Visible spectrophotometer (Thermo scientific). Ferrous ion can easily be determined by the formation of a red complex with 1,10-phenanthroline. The molar absorption coefficient at 510 nm of the complex Fe(II)-phenanthroline is equal to 11,180 mol $^{-1}$ L cm $^{-1}$.

3. Results and Discussion

3.1. Characteristics of NIO

NIO originating from Chaabet-El-Ballout (Algeria) was used as catalyst in its native form. It was only crushed and washed several times with ultrapure water and dried at 45 °C. After, it was characterized using X-ray diffraction (XRD), Raman spectroscopy, BET, X-fluorescence and SEM measurements. The DRX and Raman spectroscopy confirmed that a mineral is essentially constituted of hematite. X-fluorescence showed that the percentage of hematite is 89%, this result leads us to use this mineral as a source of iron. The BET measurement revealed that a NIO has a surface area and a total pore volume equal to $79 \text{ m}^2 \cdot \text{g}^{-1}$ and $0.08 \text{ cm}^3 \cdot \text{g}^{-1}$ respectively. the detailed of these analysis is reported in the previous work of our research team [15,16]. The SEM was investigated with a scanning electron microscopy using a Hitachi S-3400 electron microscope. A micrographs morphology (Fig. 2) indicated that the surface of NIO is compact, porous and open with a large specific surface and homogeneous distribution of grains with varying sizes, its average particle size is $1.46 \mu\text{m}$.

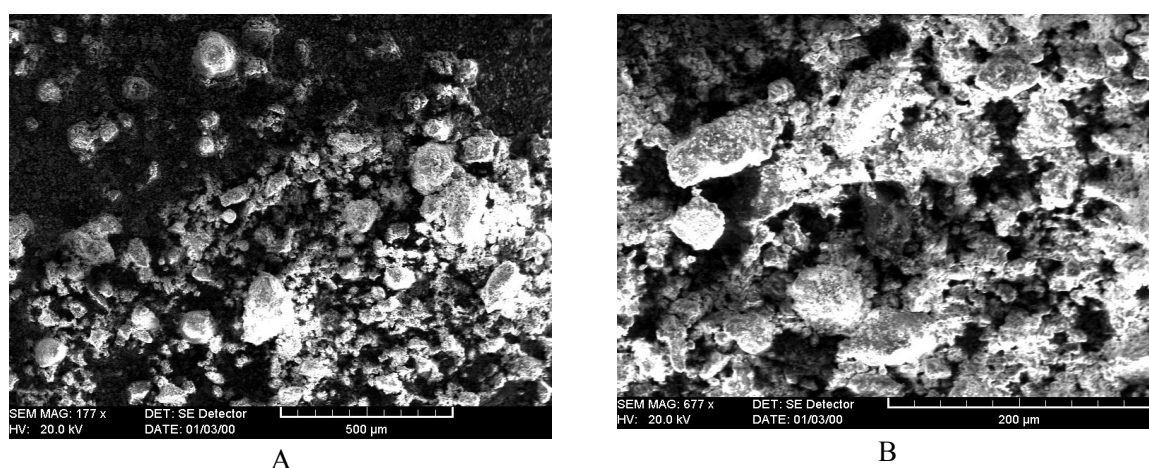


Figure 2: Scanning electron microscopic images of NIO

3.2. The kinetics disappearance of MB in the presence of different carboxylic acids

The degradation of MB (10^{-5} M) was studied in the presence of NIO ($1 \text{ g} \cdot \text{L}^{-1}$) and different concentrations of carboxylic acids in the dark and under polychromatic radiation.

3.2.1. In the dark

The results of fig.3 show that all carboxylic acids have a positive effect on the kinetic of MB degradation. Within 90 minutes, the percentages of elimination are equal to 25%, 56%, 62 % and 65% in NIO alone and in the presence of NIO/ $\text{C}_4\text{H}_6\text{O}_6$, NIO/ $\text{C}_6\text{H}_8\text{O}_7$ and NIO/ $\text{H}_2\text{C}_2\text{O}_4$ respectively. This is due to the formation of complex Fe(III)-carboxylate [17].

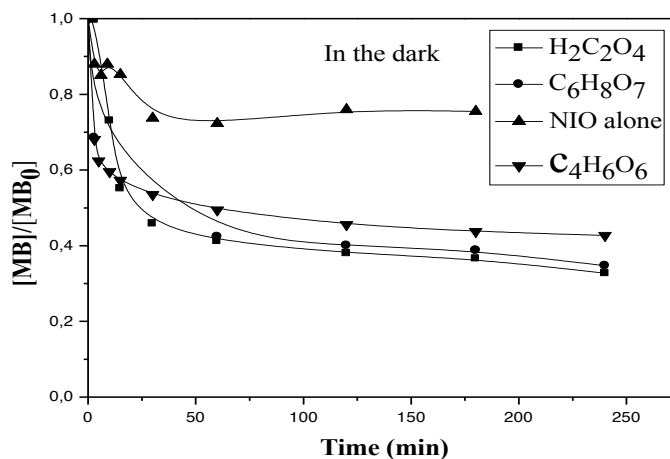


Figure 3. Degradation of MB (10^{-5} M) in the presence of $[\text{NIO}] = 1 \text{ g} \cdot \text{L}^{-1}$ and different

carboxylic acids $[C_6H_8O_7] = [C_4H_6O_6] = [H_2C_2O_4] = 4 \times 10^{-3} M$, $T = 20^\circ C$.

The different efficiency of carboxylic acids can be explained by their acidity and their capacity of forming the complexes with ferric ions. OA presents a moderate acid strength and forms Fe(III)-complexes of high stability [18,19]. That's why the best photodegradation of MB was achieved in its presence.

3.3.2. Under polychromatic irradiation ($\lambda = [300-450] nm$)

Many studies reported the effect of irradiation on the efficiency of heterogeneous Fenton and Fenton-like process. Kinetics of MB elimination were monitored in the presence of NIO ($1g.L^{-1}$) and OA, CA and TA with the concentrations varying from $10^{-3} M$ to $10^{-2}M$. The results of fig. 4 showed that the irradiation ($\lambda = [300-450] nm$) ameliorate the efficiency of natural iron oxide-carboxylic acids systems. In effect, carboxylic acids which contain the hydroxyl or carboxyl group in α position relative to carboxylic (such as: oxalic acid, citric acid and tartaric acid) form the ferricarboxylates complexes which absorb in the UVA area [17]. For a same concentration of carboxylic acid ($4 \times 10^{-3} M$), the best kinetic of MB elimination was obtained in the presence of oxalic acid (table 1), the augmentation in the concentration of carboxylic acid accelerate the kinetic of MB photodegradation whatever the nature of the acid used.

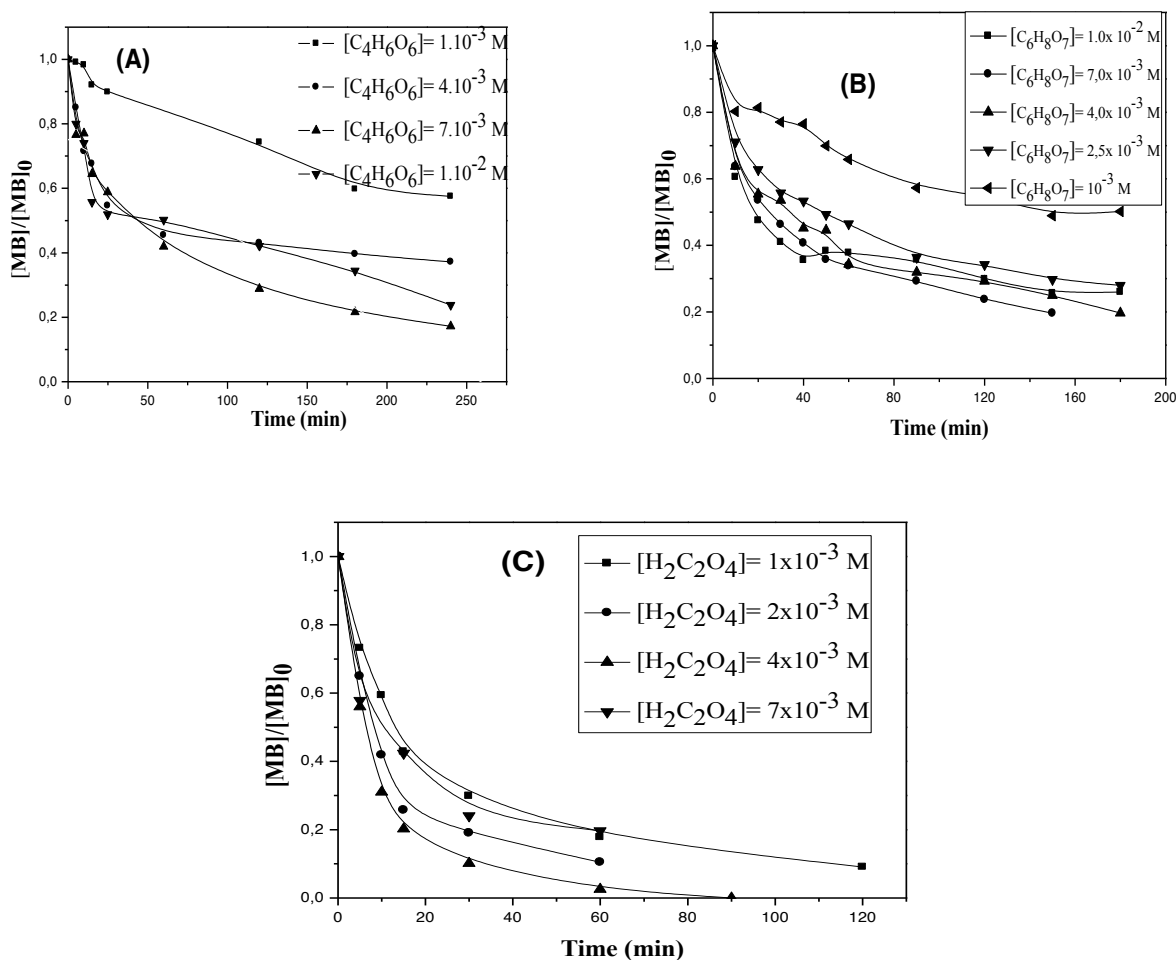


Figure 4. Effect of different carboxylic acids on the photodegradation of MB ($10^{-5} M$) in the presence of NIO ($1g.L^{-1}$) at $pH_{natural}$, $\lambda = [300-450] nm$ and $T = 20^\circ C$. A) tartric acid, B) citric acid, c) oxalic acid.

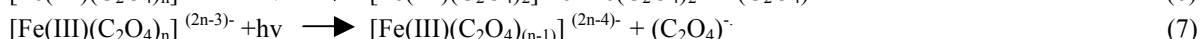
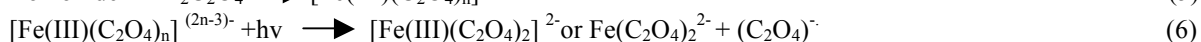
However, the optimized doses are $7 \times 10^{-3} M$ for tartaric, citric acid and $4 \times 10^{-3} M$ for oxalic acid, otherwise, any excessive reduce the kinetic of photodegradation. Within 90 min, the total photodegradation of MB was obtained in the presence of NIO and OA with a lower concentration comparatively to the other acids. The high efficiency of the NIO/OA/UV process could be attributed to the amount of dissolved Fe^{2+} . We followed the quantity of Fe(II) formed by the photodecomposition of different complexes NIO-carboxylate.

Fig. 5A shows the measurement of dissolved Fe^{2+} as a function of time in presence of OA, TA or CA. The dissolution of Fe^{2+} is fast in presence of OA. However, no dissolution of NIO in the presence of tartaric and citric acid was observed. The absence of dissolved Fe^{2+} can explain the feeble efficiency of TA and CA (fig.5A), since not enough $\bullet\text{OH}$ radicals are produced.

Table 1. Apparent rate constants and R^2 for the removal of MB in the presence of OFN and various carboxylic acids

	OA	CA	TA
k (min^{-1})	0,1076	0,0129	0,0069
R^2	0,99	0,98	0,94

The way of the production of Fe(II) and hydroxyl radicals by iron oxide/OA process is shown in the following mechanism:



In order to elucidate the involvement of $\bullet\text{OH}$ in the photocatalytic removal of MB, 2.0% *tert*-butanol was added to NIO/OA/MB (1 g.L^{-1} , $4 \times 10^{-3} \text{ M}$, 10^{-5} M) suspension irradiated under polychromatic light. From fig. 5B, we observed the total inhibition of the kinetic of MB photocatalytic in the presence of *tert*-butanol which confirm that the $\bullet\text{OH}$ radicals are the responsible species on the photodegradation of MB.

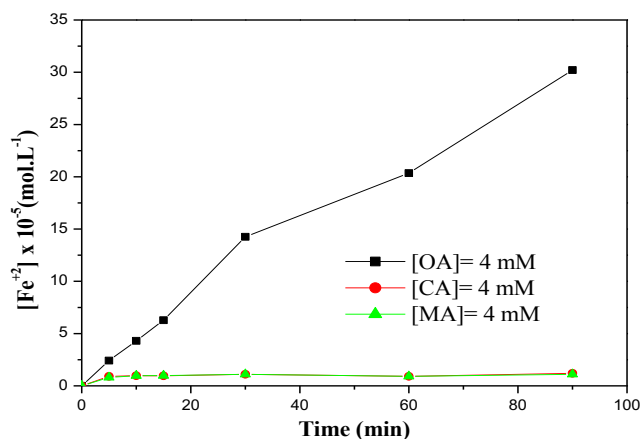


Figure 5A. Variation of dissolved Fe^{2+} vs. reaction time during the photodegradation of MB in the presence of NIO (1.0 g L^{-1}) and different acids (4 mM)

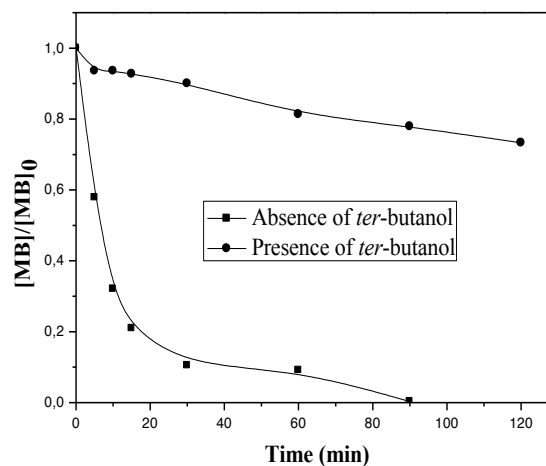


Figure 5B. Effect of *tert*-butanol on the photodegradation of MB in the presence of NIO (1.0 g L^{-1}) and OA (4 mM)

3.3. Effect of different parameters on the photodegradation of MB by NIO/OA process

3.3. 1. Effect of initial concentration of oxalate

In iron oxide–oxalate–UVA systems, the initial concentration of oxalate should be a key factor to affect the photodegradation of pollutant [9,20,21]. In order to study the effect of this parameter on the photodegradation of MB kinetics, a set of experiments were effected at the same wavelength (300–450 nm), using 1 g.L^{-1} of NIO and an initial MB concentration of 10^{-5} M . As reported in Fig. 6, an optimization of the OA dose was obtained by drawing the apparent kinetic constant of the MB degradation versus its initial concentration. The present results

show clearly that the optimum MB photodegradation was obtained by $4 \times 10^{-3} \text{ M}$ of OA under these experimental conditions. In fact, Balmer and Sulzberger[22] reported that when the concentration of oxalate is superior to $0.18 \times 10^{-3} \text{ M}$, Fe^{3+} is present, mainly, as $[\text{Fe(III)(C}_2\text{O}_4)_2]^-$ and $[\text{Fe(III)(C}_2\text{O}_4)_3]^{3-}$, this could enhance greatly MB photodegradation in the presence of OA. However, a higher concentration of oxalate, would lead to a lower initial pH at the beginning which was not favorable to photo-Fenton-like system [23]. On the other hand, excessive oxalate would occupy the adsorbed sites on the surface of iron oxide and react competitively with hydroxyl radical ($\bullet\text{OH}$) [20][9]. So, this concentration will be used to study the effect of the others parameters.

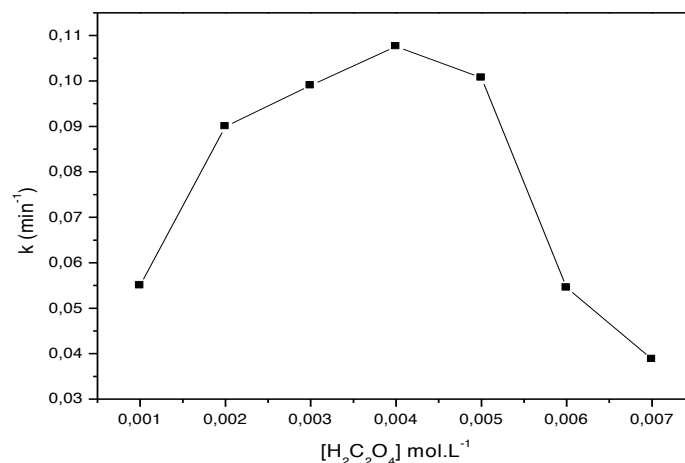


Figure 6. Effect of $[\text{OA}]_0$ on the MB (10^{-5} M) photodegradation in the presence of NIO (1 g.L^{-1}); Variation of k_{app} versus $[\text{OA}]_0$

3.3.2. The effect of the initial concentration of MB

To investigate the effect of initial concentration of MB on its degradation by NIO/OA/UV process, a set of experiments were carried out with initial concentration of MB varying from 10^{-5} to $10^{-4} \text{ mol.L}^{-1}$ in the presence of $4 \times 10^{-3} \text{ M}$ of OA and 1 g.L^{-1} of NIO and $\lambda = [300-450] \text{ nm}$ (Fig.7). It can be seen that the degradation rate decreased as initial MB concentration increased and the k_{app} values decrease significantly with the increase in the initial concentration of dye. This is due to the competition between MB and its reaction by-products for catalyst particles and it should be noted that such competition becomes more pronounced at higher concentrations. On the other hand, in the photo-Fenton-like process, the augmentation of the concentration of pollutant reduces the penetration of photons and leads to the reduction of the production of radical hydroxyl (Zheng et al. 2007). The k_{app} values were 95×10^{-4} ($R^2 = 0.95$), 0.84×10^{-2} ($R^2 = 0.99$), 1.6×10^{-2} ($R^2 = 0.98$), 1.71×10^{-2} ($R^2 = 0.99$) and 10.8×10^{-2} ($R^2 = 0.99$) min^{-1} when the initial concentration of MB were 10^{-4} , 7×10^{-5} , 5×10^{-5} , 2×10^{-5} , 10^{-5} M respectively.

3.3.3. The effect of pH

It is well known that dye wastewaters are discharged at different pH. Therefore, it is important to study the role of pH in the photodegradation of MB. Experiments were conducted at a pH range from 2 to 6 which was adjusted by titrating diluted NaOH (basic medium) or HClO_4 (acidic medium) before reaction. The initial concentration of MB, NIO and OA were respectively fixed at $10^{-5} \text{ mol.L}^{-1}$, 1 g.L^{-1} and $4 \times 10^{-3} \text{ M}$. The results are illustrated in Fig. 8. The results reported in figure 8, show that the photodegradation of MB depends strongly on pH value. Obviously, the excellent degradation of MB was obtained at pH around 3, at this pH, the most important Fe(III)–oxalate species were $\text{Fe(III)(C}_2\text{O}_4)_2^-$ and $\text{Fe(III)(C}_2\text{O}_4)_3^{3-}$, which are highly photoactive and lead to the formation of great quantity of hydroxyl radicals. When the initial pH values were beyond 4, the degradation of MB was significantly inhibited because of the low photoactivity of $\text{Fe(III)(C}_2\text{O}_4)^+$ and $[\text{Fe(III)(C}_2\text{O}_4)]^+$ species where are predominant at this interval of pH. It should be noted that MB was almost not degraded when the initial pH value was above 6 because the predominant Fe(III) species were converted to precipitate Fe(OH)_2 and Fe(OH)_3 [24,25]. The initial pH value is therefore a very important factor affecting the photo-Fenton-like reaction and in our conditions, the optimal initial pH value for the photodegradation of MB is around 3.

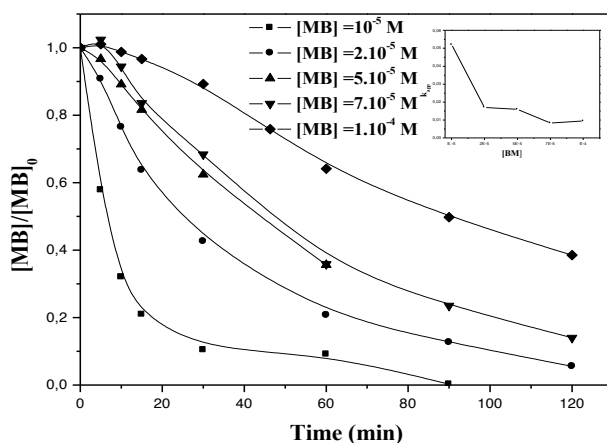


Figure 7. Effect of $[MB]_0$ on its degradation ($[OA]=4$ mM, $[NIO]=1$ g L⁻¹) under UVA irradiation ($\lambda = [300-450]$ nm) . In inset: Variation of k_{app} of MB photodegradation as function to its initial concentration.

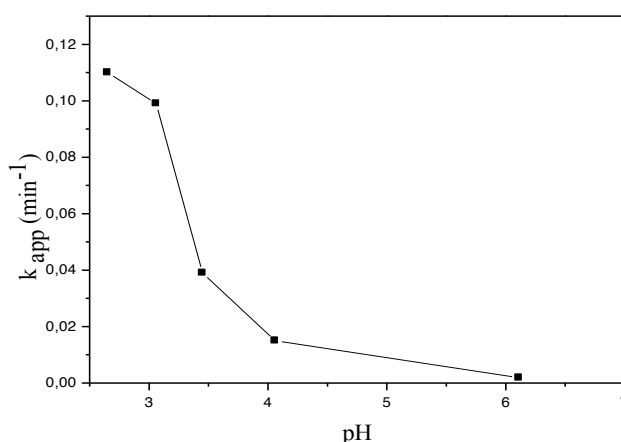


Figure 8.Effect of initial pH value on the degradation of MB (10^{-5} M) using NIO (1.0 g L⁻¹) in the presence of OA (4×10^{-3} M) under UVA irradiation.

3.3.4. The effect of different light source.

In order to investigate the effect of different artificial light and examine the efficiency of MB removal from water when the degradation is photoinduced by NIO and OA in environmental conditions. A solution of MB (10^{-5} M) was irradiated in the presence of NIO (1g.L^{-1}) and OA (4×10^{-3} M) in the laboratory ($\lambda = 310$ nm, $\lambda = 365$ and $\lambda = [300-450]$ nm) and in the laboratory station in summer day. The experimental data were well fitted by the pseudo-first-order kinetic model and the pseudo-first order kinetic constants (k_{app}) for the photodegradation of MB obtained with different light source are reported in table 2.

Table 2. Apparent rate constants for MB photodegradation under different light source.

Radiation source	310 nm	365 nm	300-450 nm	Solar light
k (min ⁻¹)	0.072	0.033	0.108	0.174
R ²	0.96	0.91	0.99	0.97

The apparent rate constants for the degradation of MB under different light source reported in table (2), show that the photodegradation of MB under solar light is more efficient than under artificial light. This could be explained by:

- A large spectrum of this light compared to the artificial one furnished by one lamp (mono/310 nm, mono/365 nm, poly/ 300- 450 nm) [26,27].
- The high photocatalytic activity of Fe₂O₃ in visible light irradiation [28].
- Fe(III)-Polycarboxylates complexes undergoes rapid photochemical reaction under sunlight [29].

Conclusion

The performance of NIO used as catalyst without treatment or modification was proved although the photo-Fenton-like process.

The photodegradation efficiency of MB in different carboxylic acids was presented the following order: NIO-oxalate>NIO-citrate> NIO-tartrate.

Through this work we found that the optimal photodegradation of MB in the NIO/OA/UV process was achieved with 4×10^{-3} M of OA at pH around 3.

The experiments under natural irradiation demonstrate that the solar photocatalytic treatment was effective for the purification of water contaminated by dye.

Acknowledgements–The authors thank “Algerian Science and Research Ministry” for the financial support of this research.

References

1. E.J. Weber, *Environ. Sci. Technol.* 29 (1995) 1163.
2. I. Arslan, I.A. Balcioglu, D.W. Bahnemann, *Dyes Pigm* 47 (2000) 207.
3. P. Cieřla, M. Kocot, P. Mytych, Z. Stasicka, *Mol. Catal. A. Chem* 224 (2004) 17.
4. K. Tanaka, K. Padermpole, T. Hisanaga, *Water Res* 34 (2000) 327.
5. A.N. Soon, B.H. Hameed, *Desalination* 269 (2011) 1.
6. N. Wang, T. Zheng, G. Zhang, P. Wang, *Environ. Chem. Eng.* 4 (2016) 762.
7. A.I. Zhihui, L. Lu, J. Li, L. Zhang, J. Qiu, M. Wu, *Phys. Chem. C* 111 (2007) 4087.
8. F. Velichkova, C. Julcour-Lebigue, B. Koumanova, H. Delmas, *Environ. Chem. Eng.* 4 (2013) 12142.
9. J. Lei, C. Liu, F. Li, X. Li, S. Zhou, T. Liu, M. Gu, Q. Wu, *Hazard. Mater* 137 (2006) 1016.
10. J.K. Leland, A.J. Bard, *Phys. Chem* 91 (1987) 5076.
11. S. Belattar, N. Debbache, N. Seraghni, T. Sehili, *Int. J. Chem. Reactor Eng.* 10 (2015) 1515.
12. S.O. Lee, T. Tran, B.H. Jung, S.J. Kim, M.J. Kim, *Hydrometallurgy* 87 (2007) 91.
13. C.H. Huang, A.T. Stone, *Environ. Sci. Technol* 34 (2000) 4117.
14. D. Panias, M. Taxiarchou, I. Douni, I. Paspaliaris, A. Kontopoulos, *Hydrometallurgy* 43 (1996) 219.
15. H. Mechakra, T. Sehili, M.A. Kribeche, A.A. Ayachi, S. Rossignol, C. George, *Photochem. Photobiol. Chem* 317 (2016) 140.
16. M.E.A. Kribęche, H. Mechakra, T. Sehili, S. Brosillon, *Environ Technol* 37 (2015) 172.
17. E.M. Rodríguez, G. Fernández, N. Klammerth, M.L. Maldonado, P.M. Álvarez, S. Malato, *Appl. Catal. B Environ* 95 (2010) 228.
18. R. Chiarizia, E.P. Horwitz, *Hydrometallurgy* 27 (1991) 339.
19. V.R. Ambikadevi, M. Lalithambika, *Appl. Clay Sci* 16 (2000) 133.
20. F.B. Li, X.Z. Li, X. M. Li, T. X. Liu, J. Dong, *Colloid Inter. Sci* 311 (2007) 481
21. Q. Lan, F.B. Li, C. X. Sun, C. S. Liu, X. Z. Li, *Hazard. Mater* 174 (2010) 64.
22. B.M. Balmer, B. Sulzberger, *Environ. Sci., Technol* 33 (1999) 2418.
23. L. Lunar, D. Sicilia, S. Rbio, D. Perez-Bendito, U. Nickel, *Water Res.* 34 (2000) 1791.
24. F. Gulshan, S. Yanagida, Y. Kameshima, T. Isobe, A. Nakajima, K. Okada, *Water. Res* 44 (2010) 2876.
25. R.M. Cornell, U. Schwertmann, Wiley–VCH, Weinheim (2003) 29.
26. M. Pérez, F. Torrades, X. Domènech, J. Peral, *Water Res.* 36 (2002) 2703.
27. H.L. Zheng, X.Y. Pan, X.Y. Xiang, *Hazard. Mater.* 141(2007) 457.
28. T. Kawahara, Y. Keichi, T.J. Hiroaki, *J. Colloid Interface Sci.* 294 (2006) 504.
29. N. Seraghni, Contribution des complexes organiques de Fe(III) dans la photodegradation de polluants organiques en solution aqueuse. Doctorat thesis. University of Constantine 2016.

(2018) ; <http://www.jmaterenvirosci.com>